fibers

MDPI

Article

Field-Calibrated Degradation Kinetics of Steel Fiber-Reinforced Shotcrete in Humid Underground Silver Mines

Omar Alejandro Guirette-Barbosa [1,2,*], Selene Castañeda-Burciaga [1,2,*], José Alberto Vela-Dávila [1], Oscar Cruz-Domínguez [1], José Luis Carrera-Escobedo [1,2], Jesús Velázquez-Macías [1], Claudia Guadalupe Lara-Torres [1], José María Celaya-Padilla [2,*], Héctor Antonio Durán-Muñoz [3] and Raúl Alejandro Velázquez-Luna [1]

[1] Department of Industrial Engineering, Universidad Politécnica de Zacatecas, Plan de Pardillo s/n, Parque Industrial, Fresnillo 99059, Zac., Mexico; veladavila@upz.edu.mx (J.A.V.-D.); ocruz@upz.edu.mx (O.C.-D.); jcarrera@upz.edu.mx (J.L.C.-E.); jvelazquez@upz.edu.mx (J.V.-M.); clara@upz.edu.mx (C.G.L.-T.); rvelazquez@upz.edu.mx (R.A.V.-L.)

[2] Postgraduate Department, Universidad Autónoma de Fresnillo, Carretera Federal Panamericana, Lindavista, Ejidal 4, Fresnillo 99039, Zac., Mexico

[3] Department of Electrical Engineering, Universidad Autónoma de Zacatecas, Alameda García Cadena 414, Zacatecas 98000, Zac., Mexico; hduran@hotmail.com

* Correspondence: omarguirette@upz.edu.mx (O.A.G.-B.); scastaneda@upz.edu.mx (S.C.-B.); jose.celaya@uaz.edu.mx (J.M.C.-P.)

Highlights

What are the main findings?

- After continuous laboratory exposure (95–100% RH, 23 ± 2 °C), steel fiber-reinforced shotcrete exhibited coordinated degradation that followed approximately first-order kinetics across compressive strength, splitting tensile strength, and mean single-fiber pull-out force. After 12 months of exposure, compressive strength decreased by 22.0%, splitting tensile strength by 21.4%, and mean single-fiber pull-out force by 26.3% ($R^2 \geq 0.99$). Core samples extracted from three underground silver mines after approximately 12 months of service showed a pooled compressive-strength loss of 9.0% compared with the mean 48 h production-control strength.

What are the implications of the main findings?

- The findings support durability-based quality control that combines standard early-age compressive-strength acceptance with periodic in-service verification and, where feasible, direct assessment of fiber pull-out or post-cracking performance. The preliminary laboratory-to-field acceleration factor, AF ≈ 2.7 (2.4–3.0), offers a practical approach for screening humidity-related deterioration. However, it should be carefully calibrated for each mine according to its specific materials, exposure conditions, and construction practices before being used to inform service-life decisions.

Abstract

Typical specifications for steel fiber-reinforced shotcrete primarily focus on early-age mechanical properties and do not provide much guidance on evaluating changes in capacity over time, particularly under humid underground service conditions. In addition, accelerated laboratory durability tests are rarely calibrated against measurements obtained from underground structures in service. This study addressed that gap with a 12-month dual-track approach: (i) maintaining controlled near-saturated conditions in the laboratory at 23 ± 2 °C and 95–100% relative humidity, with subsequent evaluation of the mechanical

Check for updates

Academic Editor: Catalin R. Picu

Received: 20 July 2026
Revised: 25 August 2026
Accepted: 31 August 2026
Published: 2 September 2026

Copyright: © 2026 by the authors. Licensee MDPI, Basel, Switzerland. This article is an open access article distributed under the terms and conditions of the Creative Commons Attribution (CC BY) license.

properties (compressive strength, splitting tensile strength, and single-fiber pull-out resistance) at 0, 3, 6, 9, and 12 months; and (ii) monitoring the compressive strength in three operating underground silver mines in Zacatecas, Mexico, using the mean 48 h production-control strength as the field reference and cores taken after approximately 12 months of service. The three laboratory trajectories were well described by first-order exponential models ($R^2 \geq 0.99$) throughout the 12-month monitoring period. The observed reductions were 22.0% for compressive strength, 21.4% for splitting tensile strength, and 26.3% for single-fiber pull-out resistance. The apparent pull-out rate constant was approximately 18% higher than the compressive-strength rate constant, though the mechanism for this difference was not identified independently. In the field, there was an apparent reduction in compressive strength of 8–10% after about 12 months. Comparison of the chamber and field compressive-strength rates produced an apparent acceleration factor, AF $\approx$ 2.7, with a per-mine range of 2.4–3.0. The high pairwise correlations among the three laboratory properties ($r \geq 0.996$) and the first PCA component, which explained 99.8% of their standardized trajectory variance, reflected closely aligned temporal trends. However, since these were based on five exposure-age means, they should be considered only exploratory evidence of co-variation rather than causation. MANOVA demonstrated significant multivariate effects on the combined compressive and splitting tensile responses across exposure ages ($p < 0.001$). The proposed acceleration factor is preliminary and restricted to the materials, sites, exposure context, and observation period studied. Routine compressive-strength core testing may be useful as a practical screening indicator, but it cannot quantitatively replace direct bond or post-cracking evaluation.

Keywords: steel fiber-reinforced shotcrete; durability; degradation kinetics; accelerated aging; field monitoring; acceleration factor; underground mining; ground support

1. Introduction

1.1. Shotcrete as a Structural Support Method in Underground Construction

In underground mining, shotcrete is typically regarded as a rapid and conformable surface support that can be applied to irregular rock surfaces immediately after excavation. Wet-mix shotcrete is frequently used in conjunction with rock bolts to limit the loosening of rock blocks within ramps, access tunnels, and working areas [1–3]. After this initial period, the performance of the shotcrete is seldom considered, yet it is of great importance. Current characterization practices focus mainly on initial and 28-day properties used to verify conformity with mechanical-performance requirements. However, the long-term properties of shotcrete, especially its retention of mechanical capacity under the humid conditions found in underground applications, have received comparatively less attention [4,5].

1.2. Fiber Reinforcement and Its Central Role in Fiber-Matrix Bond

Steel fibers enhance the post-cracking behavior of shotcrete by bridging cracks and transferring stress across the cracks, which leads to greater toughness, ductility and residual capacity [4–8]. For hooked-end steel fibers, this contribution results from mechanical anchorage, adhesion, and friction forces along the embedded fiber. Therefore, the condition of the fiber–matrix interface plays an essential role in the mechanical behavior of shotcrete reinforced with steel fibers.

This interfacial behavior is difficult to measure in an existing underground support system. Routine quality-control and service assessments of underground support systems rely mainly on matrix-related properties, particularly compressive strength, whereas the

evolution of fiber pull-out resistance is rarely measured. It has been shown that both aging and corrosion can affect the post-cracking performance of fiber-reinforced shotcrete, even when conventional strength measurements do not capture changes at the interface [9].

1.3. Degradation of Shotcrete in Humid Underground Environments

Due to the nature of the underground mining environment, there are several negative influences on the properties of shotcrete arising from a complex combination of site-specific aggressive factors. Poorly ventilated underground workings can reach high relative-humidity levels and, under some operating conditions, approach saturation. Free water may also be present because of groundwater infiltration, leakage, drilling, and production activities, while dissolved sulfates and chlorides may be transported through groundwater or seepage water [10–12].

Exposure to humid underground conditions can foster various decay processes operating through transport and reaction-controlled mechanisms in cement-based materials, which include leaching and decalcification of hydration products, carbonation mechanisms, sulfate-induced expansion, and micro-cracking resulting from changes in environmental conditions [13–15]. Shotcrete is likely to be especially vulnerable, as set accelerators modify the porosity of the matrix and its hydration products; additionally, the stratification and rebound-affected zones create preferential paths of transport [16,17]. These mechanisms create the environmental context for subsequent time-dependent changes in both the properties of the matrix and the properties of the fiber-matrix interface.

Research on the vulnerability of the metal fiber-matrix interface under humid exposure conditions has mostly relied on pull-out tests performed on non-sprayed concretes, and the resulting findings are not directly applicable to mining shotcrete. The studies performed on hooked-end fibers subjected to cyclic wet-dry chloride exposure have demonstrated that surface corrosion can increase the single-fiber bond strength due to corrosion-induced changes at the fiber surface, but exposure to such conditions may increase bond strength to the point at which fiber rupture occurs [18–20]. The microstructural condition of the interfacial transition zone (ITZ) is sensitive to environmental humidity, and changes in the ITZ may affect pull-out capacity and energy dissipation [21]. However, the direction and magnitude of the resulting bond changes depend on the exposure regime, matrix composition, fiber geometry, and the presence of cracks or aggressive ions.

Overall, these studies illustrate how environmental exposure may influence fiber–matrix bond behavior. Yet, most interface studies are conducted with cast concrete or cementitious samples subjected to chloride exposure, wet–dry cycles, or controlled curing conditions [18–21]. These studies provide important mechanistic evidence of how environmental exposure can modify fiber–matrix bond behavior. However, their findings cannot be transferred directly to steel fiber-reinforced shotcrete used under persistently humid underground mining conditions. None of these studies have paired interfacial measurements with parallel field observations and laboratory-to-field degradation-rate calibration.

1.4. The Normative Gap: Durability Without a Time Axis

Current sprayed-concrete specifications provide requirements concerning production, initial mechanical performance, fiber content, and energy-absorption classification. EN 14487-1 [22,23] specifies the performance and conformity requirements, while ACI 506R-16 [24] outlines guidelines regarding the materials, application, and quality control. However, none of these documents sets time-dependent strength-retention coefficients or a method for converting mechanical degradation measured under accelerated humid exposure into expected mechanical-property loss under underground service conditions.

This represents a normative gap with respect to the temporal evolution of mechanical capacity, not an absence of durability requirements in general.

1.5. The Methodological Gap: Uncalibrated Accelerated Aging

Accelerated aging is widely used to obtain durability data within a practical timeframe by exposing materials to simulated extreme conditions and relating changes to their performance in service. The utility of such testing depends on calibration, as it is difficult to quantify the severity and conservatism of the accelerated condition without field data [25–27]. This need for calibration poses the methodological problem addressed in this study.

Prior research has examined aspects of this issue, such as the on-site performance of fiber-reinforced shotcrete, long-term strength gain, accelerator effects, and fiber–matrix bond properties under environmental exposure [8,9,17–22,28]. However, these aspects have often been examined in isolation. To define this methodological gap, eight directly comparable studies were classified according to material, exposure condition, properties measured, inclusion of field observations, longitudinal coverage, and lab-to-field calibration, as outlined in Table 1.

Table 1. Comparison of directly related studies and the methodological components addressed.

Study	Material and Context	Field Observations	Longitudinal Degradation	Laboratory-to-Field Acceleration Factor
Monteiro et al. [8]	Steel- and polypropylene-fiber-reinforced shotcrete in an underground mine	Yes	No	No
Bernard [9]	Fiber-reinforced shotcrete	No field campaign	Yes	No
Manquehual et al. [17]	Steel fiber-reinforced shotcrete in a subsea road tunnel	Yes	Retrospective	No
Marcos-Meson et al. [18]	Steel fibers embedded in cracked concrete	No	Yes	No
Wang et al. [19]	Cracked steel fiber-reinforced concrete	No	Yes	No
Zhang et al. [21]	Steel fibers embedded in cement matrices	No	Yes	No
Yun et al. [22]	Steel fiber-reinforced shotcrete and cast concrete	No	Yes	No
Külekçi [28]	Synthetic fiber-reinforced shotcrete	Yes	No long.	No
Present study	Steel fiber-reinforced shotcrete in operating underground mines	Yes	Yes	Yes

Among the eight directly comparable studies, five examined fiber-reinforced shotcrete, three incorporated underground or field applications, and three directly evaluated fiber pull-out or fiber–matrix bond behavior. Only one study explicitly compared laboratory-prepared specimens with shotcrete produced under underground conditions [28]; however, that investigation used synthetic fibers and focused on mechanical performance without developing longitudinal degradation kinetics or an environmental acceleration factor.

None of the eight studies integrated all the following elements: steel fiber-reinforced shotcrete, longitudinal accelerated exposure, simultaneous testing of compressive strength,

splitting tensile strength, fiber pull-out resistance, parallel mechanical-property measurements in operating underground mines, modeling of property-loss kinetics, and establishment of a laboratory-to-field acceleration factor. Therefore, the identified gap is not an absence of durability studies, but the lack of an integrated, field-calibrated methodology connecting matrix and interface degradation under controlled exposure with mechanical-property loss under actual underground service conditions.

1.6. Context, Objectives, and Contributions of This Work

This study addresses both gaps simultaneously using a paired laboratory-field experimental design within the context of underground silver mining in Zacatecas, Mexico. Zacatecas is one of Mexico's principal silver-producing regions and contains multiple active underground mining operations [29–32]. The participating mines use wet-mix steel fiber-reinforced shotcrete as part of their support systems and exhibit persistently humid service conditions, as documented during the field campaign described in Section 2.6. Three mines in this district were selected to provide independent field observations in actual production, application, ventilation, and water-exposure conditions. The regional context defines the initial scope of applicability and validation of the study rather than its scientific novelty.

The experimental program was divided into two tracks and conducted over 12 months. In the laboratory track (ISO/IEC 17025:2017 [33] accredited), steel fiber-reinforced shotcrete was exposed to a near-saturated climatic chamber (RH = 95–100%, T = 23 $\pm$ 2 °C) and destructively tested at 0, 3, 6, 9 and 12 months for the following properties: uniaxial compressive strength (matrix capacity), splitting tensile strength (matrix cracking resistance), and single-fiber pull-out resistance (fiber-matrix interface). The field track compared early-age quality-control measurements from production shotcrete in three operating silver mines with compressive-strength measurements obtained from cores extracted from the corresponding support areas after approximately 12 months of service.

The purpose of this study was to provide a quantitative description of the time-dependent variation in the mechanical properties of steel fiber-reinforced shotcrete under controlled near-saturated exposure and to compare the resulting laboratory degradation rates with mechanical-property loss observed in operating underground mines. To accomplish this objective, four methodological contributions were pursued: (i) longitudinal characterization of compressive strength, splitting tensile strength and fiber pull-out resistance within a single experimental program; (ii) the simultaneous application of controlled laboratory exposure and field monitoring in three operating mines; (iii) the estimation of a preliminary laboratory-to-field acceleration factor based on degradation rates over the course of the experimental period; and (iv) the assessment of the usefulness and limitations of routinely measured compressive strength as an indirect monitoring indicator for mechanical properties that are less accessible.

The scientific novelty therefore lies in the integration of longitudinal matrix and interface testing with parallel observations from operating mines to obtain a preliminary field-calibrated relationship between accelerated laboratory degradation and underground service performance.

2. Materials and Methods

2.1. Experimental Design

The research encompassed a longitudinal, dual-track approach in which the strengths of each track offset the inherent limitations of the other. Laboratory exposure accelerates the process while providing control over the principal exposure variables considered in this study so that the testing can be performed destructively on replicate specimens for

each property at each specified age; nevertheless, the intensity of laboratory exposure relative to real service cannot be known in advance. In contrast, field monitoring captures actual service conditions because the material characteristics, application procedures, and environmental exposure correspond to those of the participating mines. Nonetheless, field monitoring provides limited options for property testing since only a few properties can be verified by core extraction; it is also subject to variability in operational processes. Using both experimental schemes simultaneously on similar materials over a period of a year enables the conversion of complementarity into calibration: laboratory exposure furnishes the shape and extent of the degradation model, whereas field exposure provides a coefficient that supports its connection to actual service conditions.

Track A (laboratory): Shotcrete samples are exposed to a controlled humid environment over a year and destructively tested at 0, 3, 6, 9, and 12 months. Three mechanical properties were selected to characterize the composite at complementary structural levels: uniaxial compressive strength represents the properties of the bulk matrix and constitutes the principal property used for its quality control; splitting tensile strength represents the resistance of the matrix to crack formation which is closely related to the transition from the pre-cracking to the post-cracking condition; and steel fiber-matrix bond, evaluated through single-fiber pull-out testing, represents the stress-transfer mechanism responsible for post-cracking resistance. The selected sampling ages define equal intervals throughout the exposure period; meanwhile, a two-point scheme (0 and 12 months) allows estimation of the overall reduction but fails to distinguish among linear, exponential, or stabilizing kinetic patterns; thus, the use of five sampling points permits model fitting and residual analysis.

Track B (field): the strength evolution of production shotcrete was monitored in three operating silver mines located underground in Zacatecas, Mexico, by comparing early-age quality-control measurements obtained during application with measurements from cores extracted at the same headings approximately 12 months later. Three mines, rather than one, were deliberately selected because with only one site, any observed decline could be attributed to site-specific differences in mixture proportions, application technique, or microenvironmental conditions; thus, including three sites, each served by different suppliers and application personnel, allows the consistency of the observed trend to be evaluated across different operational conditions, suppliers, and application crews. Track A characterizes kinetics under controlled near-saturated conditions, while Track B captures behavior under actual operating conditions, thereby allowing calculation of an acceleration factor (see Section 2.6).

The experimental program consisted of four distinct mix designs (Table 2). One reference mixture was made solely for the laboratory track, with 400 kg of cement per cubic meter. Regarding the field track, three different production mixtures were used, each supplied independently at one participating mine. Although the field mixtures had different compositions, they were required to meet the same performance specification, namely a cement content of 400–420 kg/m^3 and a target compressive strength of 250 kg/cm^2 (approximately 24.5 MPa) at 48 h. As such, the laboratory mixture and the field mixtures should not be treated as identical in terms of composition; they were compared based on normalized mechanical-property retention and apparent degradation rates, rather than absolute strength values.

Table 2. Summary of the laboratory and field experimental program.

Track	Evaluation Age	Specimen Source	Mechanical Property	Replicates	Total Tested
Laboratory	0, 3, 6, 9 and 12 months	Laboratory-prepared specimens	Compressive strength	6 per age	30
Laboratory	0, 3, 6, 9 and 12 months	Laboratory-prepared specimens	Splitting tensile strength	6 per age	30
Laboratory	0, 3, 6, 9 and 12 months	Individual specimens containing one embedded fiber	Single-fiber pull-out resistance	10 per age	50
Field	24 h	Cores obtained from production-control trays	Compressive strength	2 per location; 10 locations per mine	60
Field	48 h	Cores obtained from production-control trays	Compressive strength	2 per location; 10 locations per mine	60
Field	Approximately 12 months	Cores extracted directly from the underground shotcrete support	Compressive strength	1 per location; 10 locations per mine	30

Note: An extra thirty cores derived from the production-control trays, one per tested location, were kept as contingency cores. All specimens assigned to the mechanical tests were tested, and no specimens were discarded because of specimen damage or invalid failure modes.

2.2. Materials and Mix Proportions

The laboratory reference mixture was designed to represent the material and performance characteristics commonly required for wet-mix shotcrete in underground mining operations. It was prepared expressly under controlled laboratory conditions and was not compositionally identical to the three field production mixtures. The proportions of the laboratory reference mixture per cubic meter are presented in Table 3. The field mixtures were independently proportioned by their respective suppliers and were evaluated according to the common cement content and early-strength requirements described in Section 2.1.

Table 3. Mix proportions of the laboratory reference shotcrete per cubic meter.

Component	Specification	Dosage
Portland composite cement	CPC 40	400 kg/m^3
Washed sand	0–5 mm	850 kg
Washed fine gravel	5–10 mm	950 kg
Water	potable; w/c = 0.45	180 L
Commercial liquid set accelerator	manufacturer anonymized	4% by cement weight
Steel fibers	hooked end; length 30 mm; diameter 0.5 mm; tensile strength > 1000 MPa	40 kg/m^3

The laboratory reference mixture was prepared with CPC 40 cement supplied by one of the participating mines. The same cement type and manufacturer were used by the three independent shotcrete providers involved in the field campaign. The manufacturer and mine identities are withheld because of confidentiality agreements.

Batch-specific chemical and mineralogical characterization was not available. Therefore, the cement is identified by its commercial classification, CPC 40, and by the applicable Mexican product specification rather than by manufacturer-reported batch values.

The fine and coarse aggregates were obtained from a local source in the Emancipación area, Zacatecas, Mexico, and were supplied by an anonymized regional materials distributor. The particle-size distributions of both aggregate fractions were verified in the laboratory in accordance with NMX-C-077-ONNCCE-2019 [34] using a complete series of calibrated sieves and an automatic sieve shaker (A series of calibrated sieves, manufactured by Alcon, a civil engineering equipment supplier based in Guadalajara, Mexico, was used for the particle-size analysis). The resulting classifications confirmed a washed sand fraction of 0–5 mm and a washed fine-gravel fraction of 5–10 mm.

The relative density, water absorption, and moisture content of the aggregates were determined before batching, and the batch water was adjusted to maintain a water-to-cement ratio of 0.45 while accounting for their moisture and absorption. Although batch-level moisture-correction records were available for the laboratory mixture, comparable effective water-to-cement ratios cannot be assumed for the three field suppliers, since no equivalent moisture-correction records were available.

The selection of each component followed common regional mining practice. The cement content (400 kg/m^3) and water-to-cement ratio (0.45) correspond to the conventional usage of wet-mix shotcrete for long-distance pumping and developing early strength with an accelerator. The maximum aggregate size of 10 mm is linked to the spraying process, because larger particles cause more rebound and nozzle wear. The low-alkali accelerator at 4% by cement weight facilitates overhead application as well as the 24 h strength required for mining cycles. The hooked-end steel fibers (30 mm $\times$ 0.5 mm, aspect ratio 60, tensile strength above 1000 MPa) at 40 kg/m^3 reflect the parameters used in the three mines studied in this field campaign for headings where considerable ground movements are expected.

Mixing was performed under controlled conditions at the contractor's plant. The mixture was applied using the wet-mix method with Putzmeister equipment through a 75 mm nozzle under constant pressure (7–10 bar) by an experienced nozzleman. Spraying was preferred over casting to reproduce the relevant material characteristics because spraying provides compaction and orientation of fibers in the material whereas casting would not reproduce these effects.

2.3. Specimen Preparation and Initial Curing

Laboratory specimens for compressive and splitting tensile testing were cast directly in 150 $\times$ 300 mm cylindrical molds (The cylindrical specimen molds were manufactured by Alcon, a civil engineering equipment supplier based in Guadalajara, Mexico) and consolidated by rodding in accordance with NMX-C-159-ONNCCE-2016 [35]. The specimens were demolded approximately 24 h after casting and maintained in a controlled moist room at 23 $\pm$ 2 °C and approximately 100% relative humidity until completion of seven days of initial curing, following NMX-C-148-ONNCCE-2010 [36]. At the end of this period, the specimens assigned to the initial condition were tested to establish the 0-month reference values, while the remaining specimens were transferred to the long-term environmental chamber for testing after 3, 6, 9, and 12 months of exposure.

The Mexican NMX test methods used in this study are technically comparable to the corresponding international methods: the compression test corresponds to ASTM C39/C39M (Standard Test Method for Compressive Strength of Cylindrical Concrete Specimens. ASTM International: West Conshohocken, PA, USA, 2026) [37], and the splitting tensile test corresponds to ASTM C496/C496M (Standard Test Method for Splitting Tensile Strength of Cylindrical Concrete Specimens. ASTM International: West Conshohocken, PA, USA, 2017) [38], thereby allowing external comparison of the results.

2.4. Long-Term Exposure Conditions

The long-term exposure chamber was operated for a period of 12 months at 23 ± 2 °C, with a relative-humidity target range of 95–100%. The chamber temperature was monitored continuously by the internal thermostat and verified daily by an independent calibrated thermometer (A bimetallic thermometer with a 1 °C scale division, supplied by Alcon, a civil engineering equipment supplier based in Guadalajara, Mexico, was used for temperature monitoring). The relative humidity was sustained by continuous water nebulization in accordance with the moist-room performance parameters determined in NMX-C-148-ONNCCE-2010 [36]. However, the relative-humidity values themselves were not continuously recorded. Continuous air circulation was maintained, and the samples were kept away from direct sunlight. The samples were kept on glass supports so that they did not come in contact with any metallic surface and positioned so that their exposed surfaces remained open to the chamber environment.

These experimental conditions represent the upper bounds of humidity. They keep samples in a nearly saturated condition throughout the exposure period, while real mine tunnels undergo forced ventilation, periodic drying, and seasonal variations. This option was adopted deliberately for methodological reasons; the upper bound of humidity in laboratory conditions allows the kinetics data to be treated as a conservative envelope for the study conditions, whereas field data (Section 2.6) show how far the real condition falls below the envelope. The impact of this decision on the interpretation of the results, particularly regarding the environmental acceleration factor, is described in Section 3.4. It should be noted that experimental conditions in the chamber only simulate the humidity regime of the mining environment, while chemical agents are excluded (chlorides, sulfates, corrosive gases); the implication of this limitation is discussed in Section 4.4.

2.5. Mechanical Tests

2.5.1. Compressive Strength

Uniaxial compression tests were performed in accordance with NMX-C-083-ONNCCE-2014 [39] (same as ASTM C39/C39M). Before loading, the specimen ends were capped with molten sulfur compound in accordance with NMX-C-109-ONNCCE-2013 [40] to provide plane and parallel loading surfaces. Cylinders with a diameter of 150 mm and a height of 300 mm were tested using a calibrated 120 ton ALCON hydraulic press (equipment ID 8; nominal capacity approximately 1177 kN, Compressive strength tests were performed using 120-ton capacity compression testing machines manufactured and calibrated by Alcon, a civil engineering equipment supplier based in Guadalajara, Mexico.) at a controlled rate of 0.25 MPa/s with capped ends that allowed an even load distribution. Six cylinders were tested at each time interval to support descriptive statistics and ANOVA across exposure ages without exceeding the capacity of the environmental test chamber. The maximum load was recorded for each specimen; the failure modes were photographed and classified to confirm the validity of the test. All six scheduled specimens were tested at each exposure age, and no result was excluded. Testing was performed by a laboratory accredited by the Mexican Accreditation Entity under accreditation number C-1356-268/21 (accredited testing laboratory recognized by the Entidad Mexicana de Acreditación, A.C. (EMA), under accreditation No. C-1356-268/21) [41].

2.5.2. Splitting Tensile Strength

Splitting tensile tests were performed in accordance with the standard NMX-C-163-ONNCCE-2019 [42] (equivalent to ASTM C496/C496M). Independent 150 × 300 mm cylindrical specimens were tested using a calibrated 120 ton ALCON hydraulic press (equipment ID 7; nominal capacity approximately 1177 kN, Compressive strength tests

were performed using 120-ton capacity compression testing machines manufactured and calibrated by Alcon, a civil engineering equipment supplier based in Guadalajara, Mexico.). The cylinder was loaded by applying a diametral compressive load via bearing strips, inducing tensile stress perpendicular to the plane of loading; the splitting tensile strength was calculated from the ultimate load. Six specimens were tested at each time interval. The splitting configuration was selected because direct tension is difficult to implement for fiber-reinforced specimens.

2.5.3. Bond Between Fiber and Matrix (Single-Fiber Pull-Out)

An instrumented pull-out testing methodology was developed to determine the bond characteristics of steel fibers embedded within shotcrete matrices. The pull-out testing was based on single-fiber pull-out concepts and methods reported by other researchers [18,20]. Prismatic specimens were used for testing, using fibers with the same physical characteristics and partially exposed ends in the test specimens. The method for preparing, curing, and testing the specimens was kept constant to ensure consistent specimen and environmental histories across the three types of tests. The pull-out testing was performed using a controlled linear actuator (The single-fiber pull-out tests were performed using a Tolomatic IMA33-RN04 electromechanical linear servo actuator (Tolomatic, Inc., Hamel, MN, USA)) at a constant displacement rate of 0.5 mm/min in a quasi-static mode, so that the maximum pull-out force could be accurately determined. The axial load acting on the specimen was measured in real time using an S-type load cell (SM-5000N S-type tension/compression load cell (Interface, Inc., Scottsdale, AZ, USA)), with a maximum capacity of 5 kN and a resolution of 0.1 N. The automated system continuously recorded the load data, from which the maximum pull-out force was determined. The testing sequence involved testing ten fibers at each exposure age, providing more replicates than in the strength tests. The extracted fibers were visually examined after each test, and a photographic record of the fiber and socket was obtained, allowing assessment of oxidation and bond-surface residues. The load cell installed in the test assembly is shown in Figure 1.

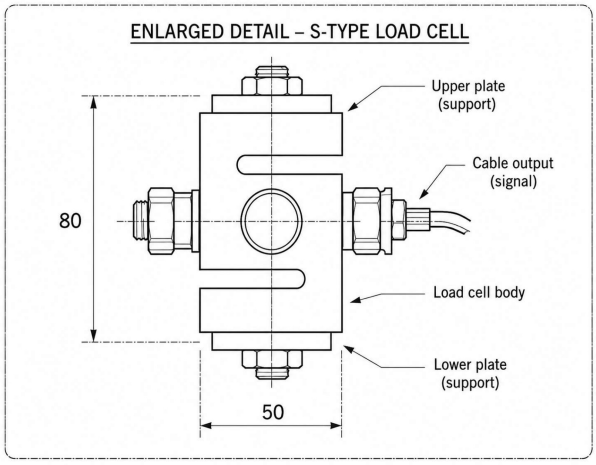


Figure 1. S-type load cell and pull-out configuration used for the fiber–matrix bond test (dimensions in mm).

2.6. Field Campaign in Three Operating Silver Mines

The data collection effort was conducted in three operating underground silver mines in Zacatecas, Mexico. Each site was served by an independent shotcrete supplier, and the supplier used a specific mixture that met the common performance criteria outlined in Section 2.1. Because of confidentiality agreements, the identities of the mine, supplier, and product are not disclosed. Ten representative locations were monitored in each mine (i.e.,

headings, ramps, access areas), for a total of 30 field locations. The sample locations were different in terms of ventilation, water inflow, mine depth, shotcrete application crew, and other operational conditions.

During the application of the shotcrete, one metal production-control tray was filled directly from the spraying equipment at each monitored location. After a minimum of twelve hours of initial setting time (i.e., hardening), each control tray was delivered to the accredited laboratory. At 24 h at least five cylindrical cores measuring 50.8 mm in diameter and 101.6 mm in length were removed from each tray, maintaining a length-to-diameter ratio of 2.0. Two cores were tested at 24 h and two at 48 h; one core was preserved as a backup specimen, if needed. The 24 h results were used for operational quality control and verification of early access safety, while the mean of the two 48 h tests was used as the initial field reference for degradation assessments. The nominal project strength targets were a compressive strength of 200 kg/cm^2 (approx. 19.6 MPa) at 24 h and at least 250 kg/cm^2 (approx. 24.5 MPa) at 48 h.

After about 12 months of service, one core was taken directly from the installed shotcrete at each of the 30 monitored locations. The field cores had nominal diameters of 38.1 mm and lengths that varied based on the actual shotcrete thickness. The support specification required at least 50.8 mm nominal shotcrete thickness over the installed steel mesh. Core extraction and preparation were performed in accordance with NMX-C-169-ONNCCE-2009 [43] in a laboratory accredited by the Mexican Accreditation Entity (EMA accreditation C-1356-268/21). To report compressive strength, the correction factor prescribed by the standard was used when the measured length-to-diameter ratio was less than 2.0.

The laboratory reference mixture and the three field production mixtures could not be considered compositionally identical, and because their reference ages were also different, laboratory and field strength values were not compared directly. Field retention was calculated separately for each mine by normalizing the corrected core strength at 12 months against the corresponding mean 48 h production-control strength. Degradation rates were not calculated from 24 h results. After 48 h, the study design could not isolate continued hydration from environmental and operational effects; this is therefore treated as a limitation in Section 4.4.

2.7. Statistical Analysis and Kinetic Modeling

The data were analyzed using IBM SPSS Statistics v26 and Statgraphics v18, and the model fits were independently verified using SciPy (version 1.18.0 (SciPy Developers), released on 19 June 2026 and distributed through the Python Package Index). A significance level of $\alpha = 0.05$ was used for all inferential statistical tests. The analysis consisted of four main components. The first component involved running descriptive statistics for each variable and exposure interval (mean, standard deviation, coefficient of variation), which provided the basis for assessing within-group variability before inferential analysis. The second component consisted of a one-way analysis of variance (ANOVA), conducted separately for each property across the different exposure intervals to determine whether the observed values differed significantly across exposure intervals beyond random within-group variation. The third component consisted of the calculation of Pearson correlations among the exposure-age means for the properties of interest; this bivariate analysis was supplemented by two multivariate tests, one being the one-way multivariate analysis of variance (MANOVA) performed on the separate compressive and splitting tensile results obtained across the five exposure-age groups using Wilks' lambda to assess the significance of the overall change, and the other being the principal component analysis (PCA) performed on the standardized means across three properties to determine whether

the joint temporal trend could be summarized by a single component. Finally, the fourth component involved kinetic modeling using first-order exponential decay:

$$f(t) = f_0\, e^{-kt}$$

where f(t) is the property value at exposure time t (months), f_0 is the initial value, and k (month^{-1}) is the degradation rate constant obtained by least-squares fitting. Goodness of fit was evaluated using R^2 and the 95% confidence interval of k.

The exponential form was selected as a parsimonious first-order representation of the observed phenomenon: it embodies the hypothesis that the instantaneous rate of capacity loss is proportional to the remaining capacity, which is mathematically consistent with a transport-controlled process but does not independently establish that mechanism, and it is the standard baseline model in accelerated life testing of construction materials [25,27]. Its two parameters have direct model interpretations (f_0, the initial capacity; k, the apparent fractional loss rate), which is what allows rates measured in different environments to be compared as a ratio. Alternative descriptions (linear, bilinear, and Weibull-type) were considered; the quality of the exponential fits (Section 3.1) did not justify additional parameters within the 12-month window, although the discrimination among models at longer horizons is acknowledged as an open task in Section 4.4.

The laboratory-to-field environmental acceleration factor was defined as the ratio of rate constants:

$$AF = \frac{k_{chamber}}{k_{field}}$$

where $k_{chamber}$ is the rate constant obtained by fitting the multi-age chamber compressive-strength series. Because each field series contained only two measurement ages-the 48 h reference and the approximately 12-month follow-up—k_{field} was calculated analytically from the normalized retention ratio rather than estimated through multi-point regression:

$$k_{field} = -\frac{ln\left(\frac{f12}{f48h}\right)}{t}$$

where f_{48h} is the mean 48 h production-control compressive strength, f_{12} is the corrected mean compressive strength of the corresponding cores after approximately 12 months of service, and t is the actual elapsed service time expressed in months. The calculation was performed separately for each mine and for the pooled field means.

This definition follows the general logic of time-transformation methods in accelerated aging [25,26]: if two environments produce degradation trajectories of the same functional form differing only in rate, then exposure times in the two environments are related by the factor AF, and laboratory results can be mapped onto a service time axis. Finally, the field-calibrated model was used to compute strength retention factors $R(t) = e^{-k_{field}\, t}$ at reference service times, with values beyond the 12-month experimental window explicitly labeled as extrapolations. The physical state of the specimens at each extraction (microcracks, efflorescence, and spalling) was documented by visual inspection, and results were contrasted with reference values from the specialized literature to support the assessment of external validity.

3. Results

3.1. Degradation of Mechanical Properties Under Sustained Humidity

Table 4 presents the individual compressive strength results for the six replicates per interval, and Table 5 presents the corresponding splitting tensile results. Table 6 summarizes the mean single-fiber pull-out force.

Table 4. Individual compressive strength results (MPa).

Exposure Time	S1	S2	S3	S4	S5	S6	Mean	SD	Loss (%)
0 months	44.8	45.2	45.0	45.4	44.7	44.9	45.0	0.26	0.0
3 months	42.8	42.5	42.3	42.9	42.4	42.7	42.6	0.24	5.3
6 months	40.2	39.8	40.0	39.6	40.1	39.7	39.9	0.24	11.3
9 months	37.7	37.2	37.5	37.0	37.6	37.4	37.4	0.26	16.9
12 months	35.4	35.0	35.2	34.8	35.3	34.9	35.1	0.24	22.0

Table 5. Individual splitting tensile strength results (MPa).

Exposure Time	S1	S2	S3	S4	S5	S6	Mean	SD	Loss (%)
0 months	4.18	4.23	4.15	4.27	4.21	4.16	4.20	0.05	0.0
3 months	4.02	4.05	3.98	4.01	4.00	4.03	4.02	0.02	4.3
6 months	3.82	3.77	3.80	3.75	3.79	3.78	3.79	0.02	9.8
9 months	3.58	3.54	3.49	3.55	3.51	3.50	3.53	0.04	16.0
12 months	3.34	3.31	3.28	3.32	3.29	3.26	3.30	0.03	21.4

Table 6. Mean single-fiber pull-out force (n = 10 fibers per interval).

Exposure Time	Mean Pull-Out Force (N)	Loss (%)
0 months	475	0.0
3 months	440	7.4
6 months	412	13.3
9 months	385	18.9
12 months	350	26.3

All three mechanical properties decreased at each successive exposure age, with no reversal in the mean values during the 12-month period. One-way ANOVA indicated statistically significant differences among exposure ages for compressive strength ($F(4, 25) = 1542.9$, $p < 0.001$) and splitting tensile strength ($F(4, 25) = 745.3$, $p < 0.001$). These results confirm differences among the age-group means but do not, by themselves, identify the physical mechanism responsible for the observed changes. The coefficient of variation for compressive strength remained below 0.7% at all exposure ages, indicating low within-group dispersion under the laboratory specimen-preparation and testing conditions.

According to Figure 2, the distributions stayed narrow throughout the exposure period, although some slight changes in the interquartile range were evident across some intermediate and later ages. These changes may simply indicate inter-individual heterogeneity at the specimen scale, but their source cannot be determined from the mechanical results alone because porosity and fiber distribution were not separately measured herein.

The ratio between compressive and splitting tensile strength (fc/ft) remained nearly constant during the exposure period, decreasing only from approximately 10.7 at month 0 to 10.6 at month 12. This stability indicates that both measured strength properties experienced similar proportional reductions within the 12-month experimental window. However, the strength ratio alone does not demonstrate that the failure mechanism remained unchanged or confirm a dissolution-controlled degradation process. Establishing the underlying mechanism would require complementary microstructural or chemical characterization, which was outside the scope of this study.

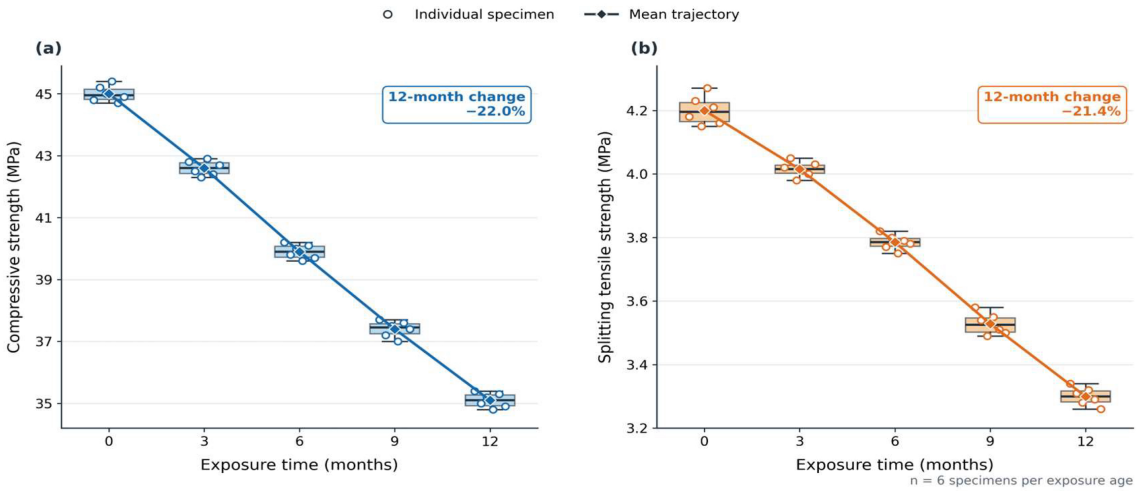


Figure 2. Distribution of (**a**) compressive strength and (**b**) splitting tensile strength by exposure interval (n = 6 per interval).

The retention factors developed in this study are based on mean mechanical-property values. They should therefore not be interpreted as characteristic design values or applied directly as code-based resistance factors. Although the within-group dispersion remained low, a reliability-based structural assessment would require a larger dataset and an explicit statistical determination of characteristic values.

Figure 3 and Table 7 presents the fitted degradation kinetics. The first-order exponential model reproduced the experimental trajectories with $R^2 \geq 0.99$ for all three properties within the 12-month observation period. The fitted initial values (f_0 = 45.1 MPa, 4.23 MPa, and 475.5 N) were close to the corresponding month 0 means, and no systematic pattern was observed in the residuals. The estimated rate constants for compressive and splitting tensile strength were 20.8×10^{-3} and 20.2×10^{-3} month^{-1}, respectively, with overlapping 95% confidence intervals. In comparison, the pull-out resistance exhibited a rate constant of 24.6×10^{-3} month^{-1}, approximately 18% higher than the compressive-strength rate constant. After 12 months, the compressive and splitting tensile properties retained approximately 78% of their initial values, whereas the pull-out resistance retained approximately 74%. These results demonstrate a faster reduction in pull-out resistance under the tested conditions; however, they do not independently identify the physical or chemical mechanism responsible for this difference because no microstructural characterization of the fiber–matrix interface was performed.

Visual inspection of the fibers revealed minor oxidation on the surface and some remaining material after 6 months of exposure. These observations are qualitative and are consistent with slow processes near the fiber-matrix interface but cannot distinguish among possible processes or confirm a specific degradation mechanism, such as corrosion of the steel, leaching, carbonation, or interfacial decalcification. Thus, the reduction in pull-out resistance should be interpreted as mechanical evidence of decreased bond performance under sustained humidity exposure rather than as definitive evidence of a specific degradation mechanism.

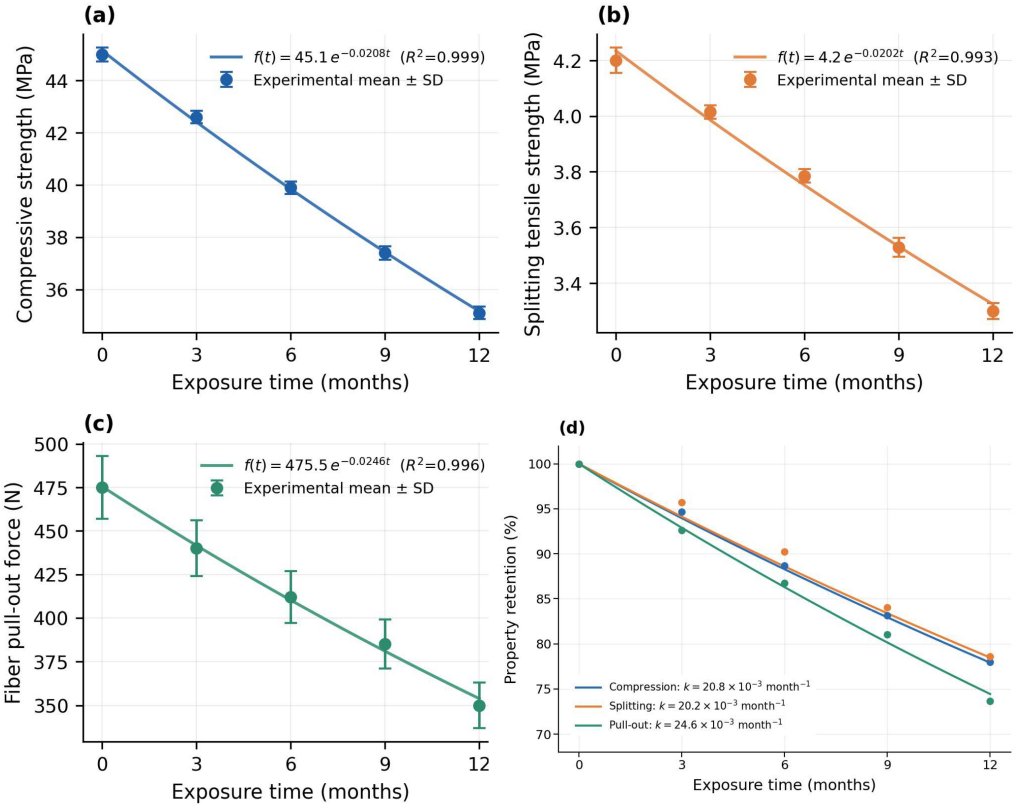


Figure 3. Degradation kinetics under sustained 95–100% RH: (**a**) compressive strength; (**b**) splitting tensile strength; (**c**) single-fiber pull-out force; and (**d**) normalized retention of the three properties with fitted first-order rate constants. Error bars: ±1 SD.

Table 7. Fitted first-order degradation parameters (0–12 months).

Property	f_0 (Fitted)	k (10^{-3} Month^{-1})	95% CI of k	R^2	Loss at 12 Months
Compressive strength (chamber)	45.1 MPa	20.8	[19.6, 22.1]	0.999	22.0%
Splitting tensile strength (chamber)	4.23 MPa	20.2	[16.8, 23.6]	0.993	21.4%
Single-Fiber pull-out resitance (chamber)	475.5 N	24.6	[22.2, 28.0]	0.996	26.3%
Compressive strength (field, pooled 3 mines)	—	7.8	6.9–8.8 [1]	—	9.0%

Note [1] Range of per-mine rate constants (Mine 1: 6.9; Mine 2: 7.9; Mine 3: 8.8 × 10^{-3} month^{-1}), computed from the mean 48 h production-control strength and the corrected mean core strength after approximately 12 months of service.

3.2. Coupled Degradation: Correlation Structure, Multivariate Tests, and Proxy Monitoring

Figure 4 and Table 8 present the Pearson correlation matrix among the interval means of the three properties. All pairwise correlations equal or exceed r = 0.996 ($p \leq 0.001$).

The strong pairwise correlations imply that the means for the three mechanical properties largely followed the same trend over the five exposure ages, but since these coefficients resulted from a shared temporal trend and a small number of interval means, they should not be construed as proof of direct causality or of a single degradation mechanism. The results show statistically significant co-variation under the conditions tested, while potential mechanisms including leaching, carbonation, corrosion, or microcracking

should remain mechanistic hypotheses until verified independently by microstructural or chemical data.

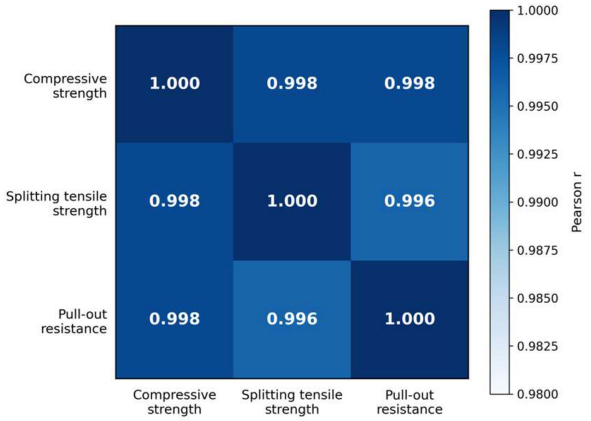


Figure 4. Pearson correlation matrix among the three mechanical properties (interval means, 0–12 months).

Table 8. Pearson correlation matrix among mechanical properties (exposure-age means).

Variable	Compressive	Splitting Tensile	Pull-Out Resistance
Compressive strength	1.000	0.998	0.998
Splitting tensile strength	0.998	1.000	0.996
Pull-out resistance	0.998	0.996	1.000

The observed co-variation has a potential practical implication for asset management because compressive strength can be evaluated in service through routine core testing, whereas splitting tensile strength and fiber–matrix bond are more difficult to measure directly in installed support. Under the laboratory conditions investigated, the ratio $k_{_pull\text{-}out}/k_{comp}$ was approximately 1.18. However, this ratio was obtained from one laboratory mixture exposed to one controlled humidity regime, and fiber–matrix bond degradation was not measured directly in the field. Consequently, compressive-strength loss should be used only as a screening indicator of possible broader mechanical deterioration, not as a quantitative substitute for bond or post-cracking performance. A relevant reduction in core strength should trigger complementary inspection or direct testing rather than an automatic conversion into an estimated bond-strength loss.

The multivariate results are summarized in Table 9. The one-way MANOVA indicated a statistically significant effect of exposure age on the joint mean vector of compressive and splitting tensile strength (Wilks' $\lambda = 0.0025$, $F(8,48) = 112.8$, $p < 0.001$; Pillai's trace = 1.303, $F(8,50) = 11.7$, $p < 0.001$). The agreement between the Wilks and Pillai criteria supports the conclusion that the combined strength response differed among exposure ages. This analysis complements the individual ANOVA results but does not establish a causal relationship between the two properties and does not include the pull-out data. Figure 5 illustrates the separation of the five exposure-age groups in the compression–splitting tensile strength plane.

Table 9. Multivariate tests of the coupled degradation.

Test	Statistic	Value	F	df	*p*
MANOVA (comp., tens. vs. exposure age)	Wilks' λ	0.0025	112.8	(8, 48)	<0.001
MANOVA (robustness)	Pillai's trace	1.303	11.7	(8, 50)	<0.001
PCA (3 properties, standardized means)	PC1 variance explained	99.8%	—	—	—
PCA (PC1 score vs. exposure time)	Pearson |r|	0.9999	—	—	—

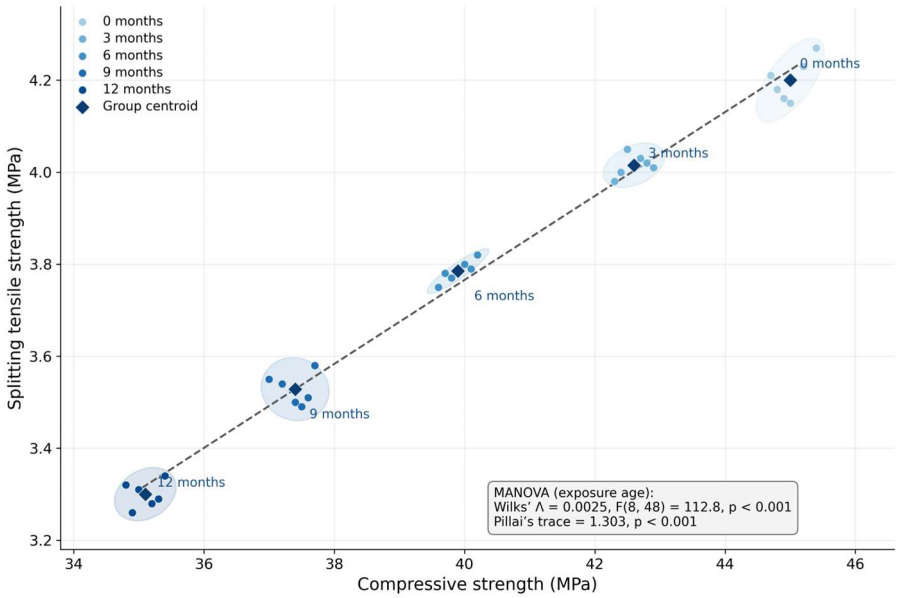


Figure 5. Joint evolution of compressive and splitting tensile strength across exposure ages (individual specimens, n = 6 per age; shaded regions: two-standard-deviation covariance ellipses per group; diamonds: group centroids). The systematic migration of the joint mean vector is the effect quantified by the MANOVA.

The PCA was used as an exploratory summary of the three standardized mechanical-property trajectories (Figure 6). The first principal component accounted for 99.8% of the variance and showed similar loadings for compressive strength, splitting tensile strength, and pull-out resistance (−0.578, −0.577, and −0.577, respectively). Its score was strongly associated with exposure time (|r| = 0.9999), indicating that the three properties shared a dominant temporal trend within the present dataset. However, the analysis was based on only five interval means and should not be interpreted as validation of a universal degradation variable or as evidence that one mechanical property can quantitatively replace the others. Its use here is descriptive and exploratory.

It is important to keep in mind the number of exposure ages when interpreting the findings from the two forms of analysis. The correlation and PCA analysis used five interval means to assess the relationships among the properties, and this likely contributed substantially to the high coefficients since all three properties changed monotonically with time. So, while these results describe the internal structure of the data at hand, they cannot be treated as precise estimates of population relationships or evidence of causality and should not be used to substantiate a quantitative proxy between mechanical properties. The MANOVA was run using the individual values from the compressive and splitting tensile tests and provides evidence that the combined compressive and splitting tensile response differed across exposure ages; however, it is not evidence for validating the relationship between fiber–matrix bond and compression. Furthermore, there is a need for more exposure conditions, other material systems, and direct measures of tensile and bond performance in the field to substantiate the theorized relationships.

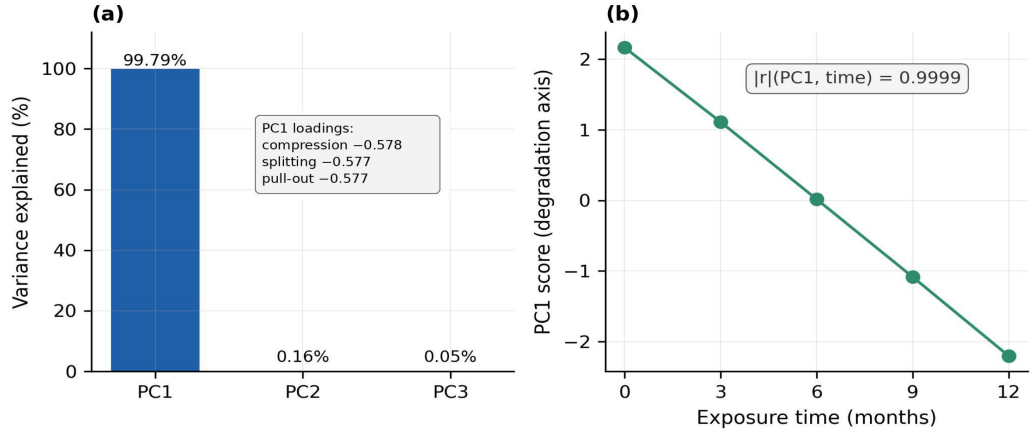


Figure 6. Principal Component Analysis (PCA) of the three degradation trajectories: (**a**) variance explained by each component, with PC1 loadings; (**b**) PC1 score versus exposure time ($|r| = 0.9999$), illustrating the dominant temporal trend identified by the exploratory PCA.

3.3. Field Campaign: Degradation in Three Operating Silver Mines

Table 10 lists the location-level mean 48 h compressive strength results from the 2025 quality-control campaign at the ten application sites per mine, and Figure 7 compares them with the strength of cores extracted from the same locations after approximately 12 months of service.

Table 10. Mean 48 h production-control compressive strength of shotcrete at ten application sites per mining unit (March 2025 campaign, ISO/IEC 17025-accredited laboratory).

Mine	Location-Level Mean Results (MPa)	Mean (MPa)
Mine 1	22.3, 20.5, 20.2, 24.1, 24.4, 20.1, 19.8, 25.7, 24.0, 23.2	22.43
Mine 2	20.2, 21.3, 18.2, 21.2, 18.9, 21.2, 20.5, 21.0, 22.3, 21.0	20.58
Mine 3	20.2, 20.1, 22.1, 23.0, 22.1, 19.2, 22.6, 19.8, 22.5, 20.9	21.25

Note: sampling sites comprise ramps, accesses, and headings at depths between levels N-420 and N-880 (Mine 1) and equivalent workings in Mines 2 and 3; the 48 h test age was established as the field reference for the degradation assessment, with each supplier dosing a set accelerator to meet the early-age target.

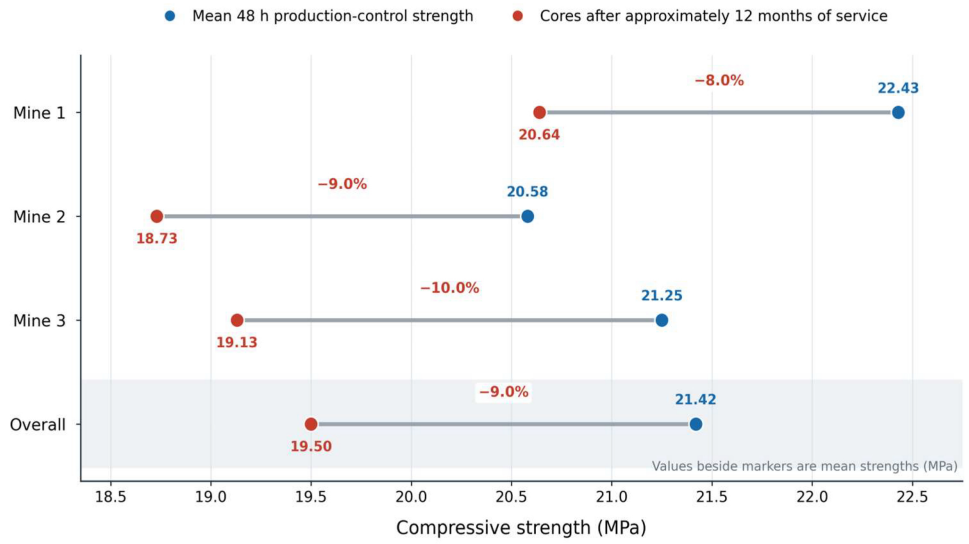


Figure 7. Compressive strength of production shotcrete in three underground silver mines: mean 48 h production-control strength versus cores extracted after approximately 12 months of service (mine means; percentage labels denote relative loss).

The mean 48 h compressive strengths were 22.43 MPa for Mine 1, 20.58 MPa for Mine 2, and 21.25 MPa for Mine 3. Although these measured means were below the nominal project target of 24.5 MPa, they represent the actual production-control performance at each mine and were therefore used as mine-specific field baselines rather than as evidence of target compliance. These values show that the three production mixtures had comparable early-age strength levels despite differences in suppliers, mixture proportions, and application crews. However, similarity in the mean values should not be interpreted as evidence that the mixtures were compositionally or statistically equivalent. Degradation was therefore calculated separately for each mine, while the pooled value was used only as an overall descriptive summary of the field campaign.

The mean compressive strength decreased from 22.43 to 20.64 MPa in Mine 1, from 20.58 to 18.73 MPa in Mine 2, and from 21.25 to 19.13 MPa in Mine 3, corresponding to apparent reductions of 8.0%, 9.0%, and 10.0%, respectively. The pooled field mean decreased from 21.42 to 19.50 MPa, representing an apparent reduction of 9.0%. The same directional change was observed in all three mines despite differences in suppliers and operating conditions. Nevertheless, the field comparison does not independently separate humidity-related degradation from continued hydration, blasting, maintenance activities, water inflow, or other site-specific influences.

The apparent field degradation rate was lowest in Mine 1 (6.9×10^{-3} month^{-1}), intermediate in Mine 2 (7.9×10^{-3} month^{-1}), and highest in Mine 3 (8.8×10^{-3} month^{-1}). These differences may reflect variations in mixture proportions, application practices, ventilation, water inflow, blasting, maintenance activities, or other site-specific conditions; their individual contributions cannot be isolated from the present field dataset. Although the field rates were lower than the chamber rate, this comparison does not demonstrate that sustained humidity was the sole or dominant cause of the observed strength reductions.

3.4. Laboratory-to-Field Transfer: The Environmental Acceleration Factor

Figure 8 superimposes the normalized chamber and field compressive-strength trajectories. The ratio between the chamber rate constant and the pooled field rate constant produced an apparent acceleration factor, $AF = k_{chamber}/k_{field} = 20.8/7.8 \approx 2.7$, with a per-mine range of 2.4–3.0. This value represents a preliminary empirical calibration for the materials, exposure conditions, and approximately 12-month observation period investigated. It should not be interpreted as a universal conversion factor for other shotcrete mixtures, mines, environmental conditions, or longer service periods.

Within the fitted model, applying $AF \approx 2.7$ would correspond to approximately 32 months of field service for 12 months of chamber exposure. However, this time conversion extends beyond the approximately 12-month field observation period and must therefore be regarded as an extrapolation rather than a directly validated equivalence. During the common 12-month observation window, the chamber compressive-strength loss was approximately 22%, whereas the pooled apparent field loss was approximately 9%. The chamber trajectory may consequently be used as a conservative experimental reference for the conditions investigated, but not as a code-based design limit or acceptance criterion without additional long-term validation.

The difference between the chamber and field rates is consistent with the contrast between continuous near-saturated exposure in the chamber and the variable conditions of operating mines, where ventilation and intermittent surface drying occur. Nevertheless, continuous site-specific humidity histories were not recorded, and the field specimens were also influenced by differences in mixture composition, application, water inflow, blasting, and maintenance. Therefore, the apparent acceleration factor cannot be interpreted as a

direct measure of the proportion of time that the field shotcrete remained saturated. The observed per-mine range of 2.4–3.0 describes the variability of the present dataset only.

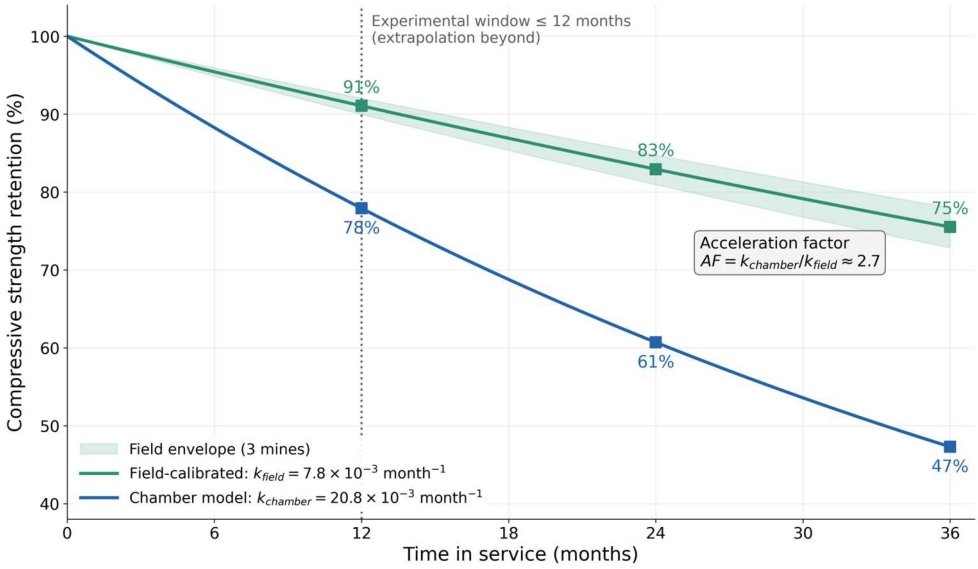


Figure 8. Laboratory-to-field transfer of degradation kinetics for compressive strength. The shaded band spans the three per-mine field rate constants; square markers indicate retention at 12, 24, and 36 months. Values beyond the 12-month experimental window are extrapolations of the fitted models.

The apparent acceleration factor may be useful for designing future extended laboratory and field monitoring programs. However, the present experiment does not validate conversions based on chamber exposures longer than 12 months or service periods extending several years. Any time equivalence beyond the common 12-month observation window should therefore be reported explicitly as a model-based extrapolation and verified through additional measurements.

Table 11 presents the compressive-strength retention factors calculated from the chamber and field rate constants. The 12-month values correspond to the experimental observation window, whereas the 24- and 36-month values are mathematical extrapolations of the fitted exponential models. The field-calibrated values are 0.91, 0.83, and 0.75 at 12, 24, and 36 months, respectively, while the chamber-derived values are 0.78, 0.61, and 0.47. These projections illustrate the effect of the different fitted rates but should not be used as validated long-term design factors. Bond-retention values were not projected from the field compressive-strength model because fiber–matrix bond was not measured directly in the operating mines.

Table 11. Model-calculated compressive-strength retention factors $R(t) = e^{-kt}$ based on the chamber and field rate constants.

Service Time	Field-Calibrated Model, $k = 7.8 \times 10^{-3}$ Month^{-1}	Chamber Model, $k = 20.8 \times 10^{-3}$ Month^{-1}
6 months [1]	0.95	0.88
12 months	0.91	0.78
24 months [1]	0.83	0.61
36 months [1]	0.75	0.47

[1] The 6-month field value is a model estimate within the observation window; the 24- and 36-month values from both models are extrapolations beyond the 12-month experimental period and require long-term validation.

4. Discussion

4.1. Degradation Mechanisms and the Vulnerability of the Fiber–Matrix Interface

The similar rates observed for compressive and splitting tensile strength are consistent with a broad deterioration of the cementitious matrix under sustained humidity exposure. However, similar trends in mechanical values do not necessarily represent a common physical or chemical degradation mechanism. The qualitative observations of white deposits, surface residues, and mild fiber oxidation after 6 months are consistent with the same processes reported for cementitious materials in humid environments, including leaching, carbonation, and microcracking [10,13,14,17]; however, these processes were not explicitly determined in the current study. Similarly, the exponential fit describes the measured mechanical behavior during the 12-month period but should not be understood as direct evidence of transport-controlled degradation. To assess the relative importance of these potential mechanisms, microstructural and chemical analysis would have to be performed.

The higher apparent rate of pull-out resistance *loss* ($k_{_pull\text{-}out}/k_{_comp} \approx 1.18$) is an important mechanical finding. Previous single-fiber pull-out studies under wet–dry chloride exposure have reported that moderate rust formation may initially increase bond through surface roughening, with deterioration occurring at more advanced corrosion stages [18–20]. The monotonic reduction measured in the present study, together with only slight visible oxidation, differs from that reported behavior. Nevertheless, the available evidence is insufficient to determine whether the difference resulted from interfacial decalcification, matrix softening, reduced frictional interlock, corrosion products, or another process. Alteration of the more porous interfacial transition zone provides a plausible explanation based on previous literature [21], but it remains a hypothesis requiring microstructural and chemical verification.

The higher rate of pull-out resistance loss indicates that the bond-related response was more sensitive under the sustained-humidity laboratory conditions than the compressive and splitting tensile responses under the same conditions. This result is qualitatively consistent with previous observations that aging may affect the post-cracking behavior of fiber-reinforced shotcrete [9]. However, a single-fiber pull-out test does not quantify full-scale ductility, energy absorption or structural reliability. The practical implication is that routine compressive-strength testing may not detect all bond-related effects, and it should be supplemented with some form of inspection or direct performance testing where deterioration is suspected.

4.2. Comparison with the Literature

The 12-month laboratory losses measured in this study, ranging from approximately 21% to 26%, are of a comparable order but slightly higher than the values of approximately 15–20% reported for fiber-reinforced cementitious materials under wet or chemically aggressive exposure [44,45]. Previous studies have also reported continued deterioration of fiber-reinforced shotcrete between one and two years, with the response depending on the accelerator and exposure conditions [22]. The somewhat larger reductions observed here may be associated with the continuous 95–100% relative-humidity regime and constant nebulization. Nevertheless, differences in mixture composition, curing, test configuration, and environmental exposure prevent a direct quantitative comparison or confirmation that the same degradation mechanisms governed all studies.

Previous laboratory–field studies have primarily examined early-age or 28-day properties [28], site-specific design characterization [8], or retrospective analyses of field observations conducted separately from laboratory aging programs [17,22]. The main advancement in the current research is the simultaneous use of controlled 12-month exposure and field observations in three operating mines, allowing comparison of normalized compressive-

strength rates over a common observation period. The resulting acceleration factor provides an initial empirical quantitative link between the laboratory and field exposure tracks within the present dataset [25–27]. However, it does not produce a generic correction for saturated chamber testing or validate multi-year service life conversions. Additional long-term paired laboratory and field exposures would be required before the relationship could be generalized for substantially longer durations.

Külekçi [28] found differences between specimens prepared and field-applied fiber-reinforced shotcrete, underscoring the impact of specimen preparation, application, and curing conditions on measured response. This paper advances the comparison by characterizing normalized time-dependent changes rather than absolute laboratory and field strength comparisons. For the 12-month time span examined, the chamber compressive-strength rate was about 2.7 times that of the pooled apparent field rate. While this result reinforces the utility of paired laboratory and field programs for interpreting accelerated exposure data, its generalizability to other materials and/or environmental conditions is limited in this investigation.

4.3. Implications for Design, Standards, and Monitoring

The current guidelines for sprayed concrete focus mainly on performance criteria at initial and early service ages, including strength, fiber content, and energy-absorption classes, among other aspects [23,24]. While they provide little guidance on how to represent changes in mechanical properties over time, Table 11 presents modeled retention values, which indicate how aging could be incorporated into future durability evaluations. The 24-month and 36-month values are modeled extrapolations and should not be applied as normative design factors in the meantime. These values might primarily be used to carry out sensitivity analyses or plan for monitoring, or to determine where additional testing would be useful. Any performance assessment models or numerical models for structural verification would require project-specific validation, with longer observation times and direct post-cracking performance assessment [46–48].

Before normative adoption, the results support a preliminary monitoring strategy for humid underground shotcrete. First, each monitored location should have a documented early-age reference strength, preferably the mean 48 h production-control value, together with its mixture, application date, supplier, and relevant environmental conditions. Second, periodic core testing can be used to compare the retained compressive strength with the location-specific baseline and identify headings that deviate from their established history. A reduction exceeding normal test variability should trigger inspection of water inflow, ventilation, visible damage, application records, and, when post-cracking performance is important, direct panel or bond-related testing rather than an inferred bond value. Third, possible mitigation measures, including improved water management, mixture optimization, corrosion-protected steel fibers, or structural synthetic fibers [44,45,49] should be selected and validated according to the specific exposure and structural requirements of each mine.

One potential pathway toward future standardization may involve the establishment of "categories of underground humidity exposure," such as ventilated-humid and continuously saturated conditions, with recommended monitoring and durability-assessment procedures outlined. The establishment of class-specific rates of deterioration will require collaborative laboratory and field data covering multiple mixtures, districts/mines, climates, geology, and practice. Such evidence would then begin to provide a basis for useful standards or recommendations associated with documents such as EN 14487-1 and ACI 506R [23,24]. In the meantime, factors determined from this research should be used to

inform research goals for the specific locations evaluated, not as normative factors or as values applicable to other designs or situations.

4.4. Limitations and Future Research

The limitations described above represent the limits within which the results can be applied and define specific points for extending the research:

(i) The experimental observation period was limited to 12 months. Consequently, the 24- and 36-month retention values presented in Table 11 are extrapolations of the fitted models rather than directly measured performance. Although five laboratory exposure ages were sufficient to evaluate the fit within the observed window, they do not establish whether the degradation rate remains constant, decreases, or is affected by a change in mechanism at longer durations. Extended laboratory and field campaigns are required to verify the long-term trajectory and formally compare alternative kinetic descriptions, including exponential, bilinear, and Weibull-type models [27].

(ii) The field baseline for the estimation of mine-specific parameters was the average production-control strength at 48 h, while the follow-up measurement was made after roughly 12 months of service. Since only these two field ages were available, the estimated per-mine rate constants are apparent two-point estimates and not independently fitted multi-age field trajectories. Continued hydration after 48 h and variations in accelerator formulation and dosage as well as other mixture-specific effects could not be disentangled from environmental and operational variables. Future work should include intermediate field ages and companion specimens stored conventionally and in-mine to separate the maturation and deterioration processes [16,22].

(iii) The chamber maintained controlled temperature and near-saturated humidity but did not simulate chlorides, sulfates, acidic groundwater, corrosive gases, thermal cycling, blasting disturbance, or sustained mechanical loading found in underground mines [10,14,15]. Additionally, the on-site observations accounted for several aspects of these operational and environmental influences without an assessment of their individual contributions. Therefore, the apparent acceleration factor cannot be attributed to humid conditions alone or easily transferred to chemically or mechanically distinct environments. Exposure to chlorides or wet-dry cycles may create a qualitatively different bond response related to corrosion and rust formation [18,19].

(iv) The study did not include SEM, XRD, chemical analysis, porosity, or quantitative microscopic characterization to investigate the fiber–matrix interfacial transition zone. Consequently, leaching, carbonation, corrosion, microcracking, and interfacial decalcification should be regarded as literature-supported hypotheses rather than mechanisms confirmed by the present observations. Future tests should implement mechanical tests and microstructural/chemical characterization at the same exposure ages to assess the relationship between pull-out resistance and changes in the matrix and interface.

(v) The field study encompassed three mines and three independent shotcrete suppliers; nevertheless, all sites were within the same mining district, and all were observed over a period of about a year. Moreover, the chamber kinetics were developed from the application of one laboratory reference mixture under one controlled exposure regime. The combination of three operations improves the assessment of consistency across the participating sites but does not establish overall applicability. Further validation should include other mixtures of shotcrete, mining districts, climates, geological settings, support configurations, and application protocols before broader applicability can be established.

5. Conclusions

This research combined a 12-month controlled laboratory exposure study with field observations in three active underground silver mines to assess time-dependent properties of a steel fiber-reinforced shotcrete lining. The laboratory track evaluated compressive-strength response, splitting tensile strength, and single-fiber pull-out resistance at 0, 3, 6, 9, and 12 months. The field track evaluated compressive strength by considering the mean 48 h production-control strength as the reference point and by extracting cores after approximately 12 months of service. Through the two tracks, normalized compressive-strength changes were compared and a preliminary laboratory-to-field calibration was derived. The main points are:

1. Under sustained near-saturated conditions (95–100% RH), all three laboratory-measured properties decreased during the 12-month period and were well described by first-order exponential models within the observed window ($R^2 > 0.99$). Compressive strength decreased from 45.0 to 35.1 MPa (−22.0%; $k = 20.8 \times 10^{-3}$ month^{-1}), splitting tensile strength from 4.20 to 3.30 MPa (−21.4%; $k = 20.2 \times 10^{-3}$ month^{-1}), and mean single-fiber pull-out force from 475 to 350 N (−26.3%; $k = 24.6 \times 10^{-3}$ month^{-1}). ANOVA confirmed significant differences among exposure ages for compressive and splitting tensile strength ($p < 0.001$). The exponential models describe the measured trajectories but do not, by themselves, establish a specific degradation mechanism or validate behavior beyond 12 months.
2. The apparent rate constant for single-fiber pull-out resistance was approximately 18% higher than that for compressive strength ($k_{_pull\text{-}out}/k_{_comp} \approx 1.18$). After 12 months, the compressive-strength response retained approximately 78% of its initial value, whereas pull-out resistance retained approximately 74%. This result indicates that the laboratory pull-out response was more sensitive under the tested exposure conditions. However, it does not directly quantify degradation of the interfacial transition zone, full-scale post-cracking performance, structural ductility, or embrittlement risk; these aspects require complementary mechanical and microstructural testing.
3. The three laboratory-measured properties showed closely aligned temporal trends. Pairwise Pearson correlations among the five exposure-age means were $r \geq 0.996$, while PCA identified a first component accounting for 99.8% of the standardized trajectory variance. MANOVA also indicated that the combined compressive and splitting tensile response differed significantly among exposure ages ($p < 0.001$). However, the correlation and PCA results are based on only five interval means and a shared monotonic time trend. They should therefore be interpreted as exploratory descriptions of co-variation, not as evidence of causality, a single physical damage mechanism, or a universal latent degradation variable.
4. Routine compressive-strength core testing can provide a practical screening indicator of time-dependent mechanical change in installed shotcrete. However, because splitting tensile strength and fiber–matrix bond were not measured directly in the field, compressive-strength loss cannot be used to quantitatively estimate their deterioration. The laboratory ratio $k_{pull\text{-}out}/k_{comp} \approx 1.18$ is specific to the reference mixture and controlled exposure investigated. A relevant reduction in field compressive strength should therefore trigger complementary inspection or direct post-cracking testing rather than an automatic conversion into an estimated bond loss.
5. Using the mean 48 h production-control strength as the field reference, the corrected compressive strength measured after approximately 12 months was lower in all three mines. The apparent reductions were 8.0% in Mine 1, 9.0% in Mine 2, and 10.0% in Mine 3, with a pooled apparent reduction of 9.0%. The corresponding two-point rate constants ranged from 6.9 to 8.8 $\times 10^{-3}$ month^{-1}, with a pooled value of 7.8 $\times 10^{-3}$ month^{-1}. The

consistent direction across the three operations strengthens the field evidence, but the design cannot isolate humidity-related degradation from continued hydration, mixture differences, blasting, ventilation, water inflow, or other operational influences.

6. Comparison of the chamber and field compressive-strength rate constants produced an apparent laboratory-to-field acceleration factor, AF ≈ 2.7, with a per-mine range of 2.4–3.0. This value constitutes a preliminary empirical calibration for the materials, sites, and approximately 12-month observation period investigated. The implied equivalence between 12 chamber months and approximately 32 field months is a model-based extrapolation rather than a directly validated service-life conversion. Therefore, the factor should not be regarded as universal or be transferred to other environments without validation, or interpreted as a direct measure of the time that field shotcrete remains saturated.
7. The field-calibrated model gave compressive-strength retention values of 0.91 at 12 months, 0.83 at 24 months, and 0.75 at 36 months. Only the 12-month value is within the observation period of the study; the 24- and 36-month values are mathematical extrapolations that would require long-term verification. These values may support sensitivity analyses and initial monitoring planning, but should not be used as normative design multipliers or code-related resistance factors. Bond retention factors could not be developed for field service, since fiber-matrix bond was not measured directly in the operating mines.

All these results pertain directly to the three participating operations in the Zacatecas mining district and give an initial framework for monitoring shotcrete in other humid underground environments. The most immediate application is establishing a location-specific 48 h reference strength followed by periodic core testing to investigate variability from that historical baseline. Compressive-strength monitoring should be used as a screening tool and complemented by direct bond or post-cracking assessment when deterioration is suspected, and wider applications of kinetic parameters, retention values, or mitigation measures require validation for each project in terms of the mixture characteristics, exposure conditions, geological setting, and structural requirements.

Aside from the quantitative results collected, the laboratory–field framework can be applied as a methodology. Other researchers, as well as mining operations, can apply synchronized controlled-exposure and field-monitoring techniques to perform site- and material-specific rate comparisons. The numerical values and fitted parameters reported here should not be transferred directly; however, replication of the paired methodology across mixtures, locations, and climates could provide the evidence needed to develop future durability-exposure classifications and monitoring guidance for steel fiber-reinforced shotcrete. This study represents a starting point toward quantitatively connecting accelerated laboratory observations with observations from underground service.

Author Contributions: Conceptualization, O.C.-D. and O.A.G.-B.; methodology, J.L.C.-E. and O.A.G.-B.; software, S.C.-B. and J.M.C.-P.; validation, J.V.-M., R.A.V.-L. and C.G.L.-T.; formal analysis, O.A.G.-B. and S.C.-B.; investigation, S.C.-B. and H.A.D.-M.; resources, O.A.G.-B. and J.M.C.-P.; data curation, J.A.V.-D., H.A.D.-M. and R.A.V.-L.; writing—original draft preparation, O.A.G.-B. and J.A.V.-D.; writing—review and editing, S.C.-B. and J.V.-M.; visualization, O.C.-D. and H.A.D.-M.; supervision, O.A.G.-B., R.A.V.-L. and J.L.C.-E. All authors have read and agreed to the published version of the manuscript.

Funding: This research received no external funding.

Data Availability Statement: The original contributions presented in this study are included in the article. Further inquiries can be directed to the corresponding authors.

Conflicts of Interest: The authors declare no conflicts of interest.

References

1. Soares, E.; Gomes, A. Inovações técnicas do concreto projetado aplicado em obras subterrâneas. In Proceedings of the Brazilian Congress of Soil Mechanics and Geotechnical Engineering, Campinas, Brazil, 15–18 September 2020. [CrossRef]
2. Aire, C.; Aguilar, L. Fiber reinforced shotcrete control tests in the Mexico City metro line 12 tunnel. *Rev. ALCONPAT* **2021**, *11*, 73–87. [CrossRef]
3. Moon, T.; Wang, E.; Oh, J.; Li, K.; Ramandi, H.; Zhang, C.; Saydam, S. Evaluation of Shotcrete Performance from Full-Scale Load-Deflection Tests Using Numerical Analysis. In Proceedings of the ARMA 57th US Rock Mechanics/Geomechanics Symposium, Atlanta, Georgia, USA, 25–28 June 2023. [CrossRef]
4. Oreste, P.; Oggeri, C.; Spagnoli, G. Fiber-reinforced shotcrete lining for stabilizing rock blocks around underground cavities. *Transp. Geotech.* **2024**, *49*, 101407. [CrossRef]
5. Xiao, S.; Yang, J.; Liu, Z.; Yang, W.; He, J. Effects of Steel Fiber Content on Compressive Properties and Constitutive Relation of Ultra-High Performance Shotcrete (UHPSC). *Buildings* **2024**, *14*, 1503. [CrossRef]
6. Zhou, F.; Zhang, B.; Pan, Y.; Zhou, Y. Mechanical Performance of Fiber-Reinforced Shotcrete for Underground Mines. *Buildings* **2025**, *15*, 3689. [CrossRef]
7. Jiang, P.; Zhang, Z.; Wang, H.; Huang, J.; Luo, X.; Xu, F. Experimental research on mechanical and impact properties of lightweight aggregate fiber shotcrete. *Constr. Build. Mater.* **2022**, *333*, 127402. [CrossRef]
8. Monteiro, V.M.A.; Silva, F.d.A. On the design of the fiber reinforced shotcrete applied as primary rock support in the Cuiabá underground mining excavations: A case study. *Case Stud. Constr. Mater.* **2021**, *15*, e00784. [CrossRef]
9. Bernard, E.S. Changes in long-term performance of fiber reinforced shotcrete due to corrosion and embrittlement. *Tunn. Undergr. Space Technol.* **2020**, *98*, 103335. [CrossRef]
10. Novikova, U.; Strokin, K.; Krasilnikova, I. Corrosion Resistance of Shotcrete under the Influence of Salt Solutions. *Constr. Mater.* **2024**, *3*, 31–36. [CrossRef]
11. Nordstrom, E. Durability of steel fibre reinforced shotcrete with regard to corrosion. In *Shotcrete: Engineering Developments*; CRC Press: Boca Raton, FL, USA, 2020. [CrossRef]
12. Jin, X.; He, J.; Hou, C.; Luo, W.; He, W. The Mechanical Properties of Early Aged Shotcrete under Internal Sulfate Attack. *Materials* **2021**, *14*, 3726. [CrossRef] [PubMed]
13. Pan, H.; Qiu, Y.; Jiang, H.; Zhao, Q.; Li, N.; Wu, X. Carbonation depth assessment in shotcrete with various initial damage degrees and accelerator dosages: Experimental study. *Constr. Build. Mater.* **2023**, *404*, 133192. [CrossRef]
14. Steindl, F.; Galan, I.; Baldermann, A.; Sakoparnig, M.; Briendl, L.; Juhart, J.; Thumann, M.; Dietzel, M.; Röck, R.; Kusterle, W.; et al. Sulfate durability and leaching behaviour of dry- and wet-mix shotcrete mixes. *Cem. Concr. Res.* **2020**, *137*, 106180. [CrossRef]
15. Kaufmann, J.; Loser, R.; Winnefeld, F.; Leemann, A. Sulfate resistance testing of shotcrete—Sample preparation in the field and under laboratory conditions. *Constr. Build. Mater.* **2021**, *276*, 122233. [CrossRef]
16. Garba, M.J.; Tian, Y.; Xie, Z.; Yu, C.; Hu, C.; Chen, L.; Yuan, Q. Effect of accelerators on the long-term performance of shotcrete and its improvement strategies: A review. *J. Build. Eng.* **2024**, *89*, 109364. [CrossRef]
17. Manquehual, C.J.; Jakobsen, P.D.; Holter, K.G.; De Weerdt, K.; Danner, T.; Bruland, A. Comparison of the condition of steel fiber-reinforced shotcrete with waterglass and alkali-free activators after more than 20 years of service in a subsea road tunnel. *Constr. Build. Mater.* **2022**, *328*, 127090. [CrossRef]
18. Marcos-Meson, V.; Solgaard, A.; Fischer, G.; Edvardsen, C.; Michel, A. Pull-out behaviour of hooked-end steel fibres in cracked concrete exposed to wet-dry cycles of chlorides and carbon dioxide—Mechanical performance. *Constr. Build. Mater.* **2020**, *240*, 117764. [CrossRef]
19. Wang, X.; Liu, Y.; Liu, S. Effect of chloride-induced corrosion on bond performance of various steel fibers in cracked SFRC. *Cem. Concr. Compos.* **2023**, *140*, 105113. [CrossRef]
20. Yoo, D.-Y.; Gim, J.Y.; Chun, B. Effects of rust layer and corrosion degree on the pullout behavior of steel fibers from ultra-high-performance concrete. *J. Mater. Res. Technol.* **2020**, *9*, 3632–3648. [CrossRef]
21. Zhang, K.; Yuan, Q.; Zuo, S.; Huang, T.; Wang, Y. Pullout behavior of steel fiber embedded into cement matrix under low humidity curing. *Cem. Concr. Res.* **2023**, *172*, 107217. [CrossRef]
22. Yun, K.K.; Choi, S.; Ha, T.; Hossain, M.S.; Han, S. Comparison of Long-Term Strength Development of Steel Fiber Shotcrete with Cast Concrete Based on Accelerator Type. *Materials* **2020**, *13*, 5599. [CrossRef] [PubMed]
23. *EN 14487-1:2022*; Sprayed Concrete, Part 1: Definitions, Specifications and Conformity. European Committee for Standardization: Brussels, Belgium, 2022.
24. *ACI 506R-16*; Guide to Shotcrete. American Concrete Institute: Farmington Hills, MI, USA, 2016.
25. Chen, Y.; Davalos, J.F.; Ray, I. Durability Prediction for GFRP Reinforcing Bars Using Short-Term Data of Accelerated Aging Tests. *J. Compos. Constr.* **2006**, *10*, 279–286. [CrossRef]
26. Starkova, O.; Gagani, A.I.; Karl, C.W.; Rocha, I.B.C.M.; Burlakovs, J.; Krauklis, A.E. Modelling of Environmental Ageing of Polymers and Polymer Composites—Durability Prediction Methods. *Polymers* **2022**, *14*, 907. [CrossRef]

27. Guo, X.; Qiao, H.; Zhu, B.; Wang, P.; Wen, S. Accelerated Life Testing of Concrete based on Three-parameter Weibull Stochastic Approach. *KSCE J. Civ. Eng.* **2019**, *23*, 1682–1690. [CrossRef]
28. Külekçi, G. Comparison of Field and Laboratory Result of Fiber Reinforced Shotcrete Application. *Period. Polytech. Civ. Eng.* **2021**, *65*, 463–473. [CrossRef]
29. The Silver Institute. World Silver Survey 2025—Silver Supply & Demand. Available online: https://silverinstitute.org/silver-supply-demand/ (accessed on 12 May 2026).
30. General Directorate of Mining Development; Ministry of Economy (Mexico). Statistical Bulletin of the Mining-Metallurgical Industry, July 2024 Edition. Available online: https://www.gob.mx/cms/uploads/attachment/file/947677/Bolet_n_estad_stico_-_julio_2024.pdf (accessed on 12 May 2026).
31. Fresnillo PLC. *Full Year 2024 Production Report*; Fresnillo PLC: Mexico City, Mexico, 2025. Available online: https://www.fresnilloplc.com (accessed on 14 July 2026).
32. U.S. Geological Survey. *Mineral Commodity Summaries 2025—Silver*; USGS: Reston, VA, USA, 2025. Available online: https://pubs.usgs.gov/periodicals/mcs2025/mcs2025-silver.pdf (accessed on 14 July 2026).
33. *ISO/IEC 17025:2017*; General Requirements for the Competence of Testing and Calibration Laboratories. International Organization for Standardization: Geneva, Switzerland, 2017.
34. *NMX-C-077-ONNCCE-2019*; Construction Industry, Aggregates for Concrete, Particle-Size Analysis, Test Method. ONNCCE: Mexico City, Mexico, 2019.
35. *NMX-C-159-ONNCCE-2016*; Construction Industry, Concrete, Elaboration and Curing of Test Specimens. ONNCCE: Mexico City, Mexico, 2016.
36. *NMX-C-148-ONNCCE-2010*; Construction Industry, Cements and Hydraulic Concretes, Cabinets, Wet Rooms and Storage Tanks, Design and Operation Conditions. ONNCCE: Mexico City, Mexico, 2010.
37. *ASTM C39/C39M*; Standard Test Method for Compressive Strength of Cylindrical Concrete Specimens. ASTM International: West Conshohocken, PA, USA, 2026.
38. *ASTM C496/C496M* ; Standard Test Method for Splitting Tensile Strength of Cylindrical Concrete Specimens. ASTM International: West Conshohocken, PA, USA, 2017.
39. *NMX-C-083-ONNCCE-2014*; Construction Industry, Concrete, Determination of Compressive Strength of Specimens, Test Method. ONNCCE: Mexico City, Mexico, 2014.
40. *NMX-C-109-ONNCCE-2013*; Construction Industry, Hydraulic Concrete, Capping of Cylindrical Specimens. ONNCCE: Mexico City, Mexico, 2013.
41. *C-1356-268/21*; Accredited Testing Laboratory Recognized by the Entidad Mexicana de Acreditación, A.C. (EMA). ONNCCE: Mexico City, Mexico.
42. *NMX-C-163-ONNCCE-2019*; Construction Industry, Hydraulic Concrete, Determination of Splitting Tensile Strength of Concrete Cylinders, Test Method. ONNCCE: Mexico City, Mexico, 2019.
43. *NMX-C-169-ONNCCE-2009*; Construction Industry, Concrete, Extraction of Cylindrical or Prismatic Specimens from Hardened Hydraulic Concrete. ONNCCE: Mexico City, Mexico, 2009.
44. Kroviakov, S.; Kryzhanovskyi, V.; Hedulian, D. Comparison of the Corrosion Resistance of Fiber-Reinforced Concrete with Steel and Polypropylene Fibers in an Acidic Environment. *Constr. Mater.* **2025**, *5*, 6. [CrossRef]
45. Mohamed, O.; Zuaiter, H. Fresh Properties, Strength, and Durability of Fiber-Reinforced Geopolymer and Conventional Concrete: A Review. *Polymers* **2024**, *16*, 141. [CrossRef] [PubMed]
46. Hammer, A.; Thewes, M.; Galler, R. Time-dependent material behavior of shotcrete—New empirical model for the strength development and basic experimental investigations. *Tunn. Undergr. Space Technol.* **2020**, *99*, 103238. [CrossRef]
47. Wang, Y.; Luo, M. Analysis of Support Reaction Curves considering Time-Varying Effect of Shotcrete. *Adv. Civ. Eng.* **2020**, *2020*, 6069432. [CrossRef]
48. Lu, J.; Li, M.; Ran, X.; Liu, L. Research on the bond-slip behavior and constitutive relationship between I-shaped steel and shotcrete in tunnel. *Struct. Concr.* **2023**, *24*, 6011–6024. [CrossRef]
49. Higuera, C.; Pulido, J.; Rodríguez, S. Evaluation of the compression behavior and physical properties of recycled PET fibers reinforced cement mortars. *Sci. Tech.* **2020**, *25*, 269–279.

Disclaimer/Publisher's Note: The statements, opinions and data contained in all publications are solely those of the individual author(s) and contributor(s) and not of MDPI and/or the editor(s). MDPI and/or the editor(s) disclaim responsibility for any injury to people or property resulting from any ideas, methods, instructions or products referred to in the content.